# FMDB Transactions on Sustainable Energy Sequence



# **Analysis of Non-Isolated Four-Port Converters with Cascaded Filter for Electric Vehicle Application**

K. Arulvendhan<sup>1</sup>, P. Srinivasan<sup>2,\*</sup>, Amal Babu<sup>3</sup>

<sup>1,3</sup>Department of Electrical and Electronics Engineering, SRM Institute of Science and Technology, Ramapuram, Chennai, Tamil Nadu, India.

<sup>2</sup>Department of Electrical and Electronics Engineering, Saveetha Engineering College, Thandalam, Chennai, Tamil Nadu, India.

arulvenk@srmist.edu.in<sup>1</sup>, srinivasp808@gmail.com<sup>2</sup>, amal.babu35@gmail.com<sup>3</sup>

Abstract: Recent improvements in power electronics have made it possible to make high-gain, step-up, non-isolated converters with low output voltage ripple. These are very important for modern DC/DC converter applications. These converters are becoming more common in electric vehicle (EV) systems, where they are needed for efficient energy interfacing. In integrated power systems, high-gain step-up multiport converters are especially useful for connecting multiple sources like photovoltaic (PV) panels, batteries, and DC loads. Closed-loop non-isolated multiport buck-boost and boost converters are used to better control the load voltage and the speed of the DC motor. This paper talks about how to design and control a closed-loop controlled multiport converter. It compares the performance of Proportional-Integral-Derivative (PID) and Model Predictive Control (MPC) strategies. We look at the control schemes using important factors like settling time and steady-state error. A small-signal model is created to help with the design and study of the suggested converter. We use MATLAB simulations to check how well the system responds to changes and how reliable it is under different operating conditions. The results show that the suggested control strategies greatly improve the converter's performance, making them suitable for use in multi-source energy systems, such as electric vehicles (EVs) and renewable energy integration, that need precise voltage regulation and quick response to changes.

**Keywords:** Interleaved Boost; Buck Boost Converter (BBC); Proportional-Integral-Derivative (PID) Controller; Model-Predictive-Controller (MPC); Steady State Analysis; R-Load and Motor Load.

Received on: 20/04/2024, Revised on: 01/07/2024, Accepted on: 03/09/2024, Published on: 09/06/2025

Journal Homepage: <a href="https://www.fmdbpub.com/user/journals/details/FTSES">https://www.fmdbpub.com/user/journals/details/FTSES</a>

**DOI:** https://doi.org/10.69888/FTSES.2025.000413

**Cite as:** K. Arulvendhan, P. Srinivasan, and A. Babu, "Analysis of Non-Isolated Four-Port Converters with Cascaded Filter for Electric Vehicle Application," *FMDB Transactions on Sustainable Energy Sequence*, vol. 3, no. 1, pp. 1–15, 2025.

**Copyright** © 2025 K. Arulvendhan *et al.*, licensed to Fernando Martins De Bulhão (FMDB) Publishing Company. This is an open access article distributed under <u>CC BY-NC-SA 4.0</u>, which allows unlimited use, distribution, and reproduction in any medium with proper attribution.

### 1. Introduction

Rising greenhouse gases, rapid increases in energy consumption, global warming, and the depletion of fossil fuels have driven the development of advanced-range vehicle technology. The automotive mobile industry thus has already started developing greenhouse gas electric (E-V) and hybrid-electric vehicles (HEV). In such a vehicle, the motor-drive system is a core module.

\*~

<sup>\*</sup>Corresponding author.

In Saafan et al. [1], a novel non-isolated four-port DC–DC converter will be used for a DC micro-grid application. The expected converters have excellent quality in projecting the DC link voltage, regardless of resource availability. Steady-state analysis is conducted from this point to determine the voltage gains across all the ports. The four ports of the converter consist of two inputs, one bidirectional port, and one output. Interrupting, charging, and discharging modes on the input side are not allowed. The detailed analysis and simulation of a four-port DC-DC converter are provided in Balaji et al. [2]. A four-port non-isolated high voltage gain converter independent of a renewable source system is discussed in Baladuraikannan et al. [3].

An interleaved boost converter voltage multiplier circuit and coupled inductors form an FOPID controller, which is proposed for a four-switch Buck-Boost DC-DC converter to reduce output power, as described in Qi et al. [4]. To miniaturise the ripple current of the inductor, a dual-trigger switch strategy is adopted as a feature. Additionally, a fractional-order PID controller is implemented for voltage module repair, using a PSO algorithm to optimise the controller's parameters. In Loganathan et al. [5], the DC-DC converters are largely major devices and are used in applications like EV (Electric vehicles), fuel cells, sustainable systems, etc. The simulated DC-DC converter is compared with other converter topologies, such as the conservative boost converter (BC), multidevice boost converter (MDBC), and two-phase interleaved boost converter (IBC), to evaluate its active performance [6].

A port DC-DC converter (MPC) of four ports for renewable energy use is shown in this study, Rostami et al. [7]. The converter comprises two boost converters and a switched-capacitor. Leveraging a bidirectional buck-boost converter, the converter charges/discharges energy storage. Under the presumed functioning of the converter, a shared ground between the input and load ports utilises the high-gain voltage and continuous current of the ports, making the converter suitable for more critical applications. In every mode of operation, the converter is a voltage-boost high-gain. It can also operate under imbalanced conditions, including varying power and value of input voltages from the sources. The input power of the sources and the output voltage vary depending on the switching policy used. The converter also operates in a cycle between charging and discharging modes. Stable Renewable Energy Sources (RES) are being used nowadays to solve environmental issues. Under high-irradiance situations, every RES that offers additional benefits, such as photovoltaic (PV) systems, is effective for power generation. They are low-maintenance, reduce pollution, and extract efficient performance, creating stable power. But using renewable energy in the DC microgrid presents some difficulties, like voltage rise, synchronising, and protection.

While single converters utilise diverse RES and storage elements to solve the problem, Multiport converters sacrifice the size and complexity of static converters, centralised controllers, and straightforward energy-management schemes. In addition, the interfacing of the storage requires a two-way power path. In this application, a multiport converter and separate multiport converters with special devices are required for linked operations and various renewable energy sources [8]. MPC-based model-predictive control provides high-efficiency operation with low static error and enhanced load regulation irrespective of group. Overall, a partially isolated converter provides soft-switching, high-power gain, and efficiency with low switching losses. Concurrently, higher power-density benefits and non-isolation circuit splitting reduce circuit size to a minimum. Because the transient operations include rapid dynamic-response, model-predictive-control (MPC) is utilised for realising the present control procedures of the two layers. Furthermore, the MPC is specifically designed to adjust to topological developments. Simulations and `experimentally` test the expected system [9].

The consequences demonstrate that, after determining the optimal operating mode based on input-source conditions, the mode-changeable converter provided here effectively completes the most preferred power path. Moreover, the control technique in Single Input Multiple Output and Multiple Input Multiple Output modes is strong and effective. Load variations, input voltage fluctuations, and reference voltage deviations are presented in the literature, Wang et al. [10], for a DC-DC buck converter system. In an attempt to enhance the tracking performance of composite voltage controllers, triggered by a model-predictive control (MPC) with a reduced-order state observer (RESO), matched and mismatched turbulence is understood as total disturbances within an artistically recommended error tracking paradigm. A RESO is thus well-developed to forecast and handle these disturbances. In like fashion, an MPC is developed to provide advanced steady-state control and enhanced system robustness. The new composite controller demonstrates the settling time property through proportional simulations, resulting in a faster and smoother response curve than the standard MPC. Moreover, during disturbance, simulated strategies show improved steady-state analysis, faster voltage-tracking, and more disturbance rejection capabilities.

# 2. Methodology

The Simulated Block Diagram of four-port bi-directional DC-DC converters in a loop system is revealed. The operation process of the four-port bidirectional DC-DC converter system involves integrating energy transfer between input sources and output loads through controlled switching processes. The PV source, as a renewable energy input, provides DC power according to solar irradiance. This power is pumped into the four-port converter and used either to supply the downstream loads directly or to charge the battery whenever generation exceeds demand. The battery source, serving as the auxiliary energy reservoir, saves energy and provides power whenever the PV input is low or zero, such as at night or during rain (Figure 1).

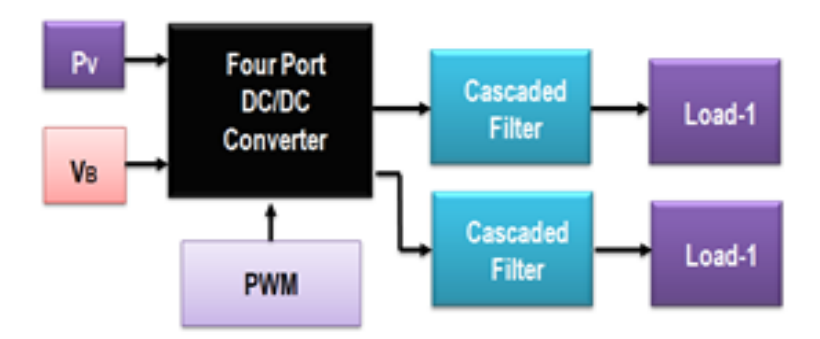


Figure 1: Proposed simulation block diagram of a port bi-directional DC-DC converter

The converter is powered by a PWM controller that governs the switching patterns of the power electronic device. Through this modulation, the power transfer is regulated to the extent that every port can supply or draw power as necessary. PWM signals are obtained from real-time feedback like load demand, PV output, and battery State of Charge (SOC). When the load requirement is higher than the PV output, the controller forces the battery to discharge and recharge the power. When the PV output exceeds the load requirement and the battery is low, the battery gets charged in the process. Cascaded filters are used in the output stage to remove any high-frequency ripples generated due to switching action. These filters provide high-quality and stable DC voltage to the loads. Both loads identified as Load-1 are supplied with filtered power, which can be controlled individually according to their respective needs.

The converter dynamically balances energy between sources and loads through bidirectional control, allowing for the complete utilisation of renewable energy and battery health, while providing continuous power to connected loads. A closed-loop Simulation block diagram of a Port Bi-directional DC-DC converter for FOPID/SMC controller systems is shown. Continuous operation of a four-port bidirectional DC-DC converter system is characterised by uninterrupted communication between multiple energy sources and loads under real-time control. First, power is provided by the photovoltaic (PV) source, which depends on the availability of sunlight, and is fed to the converter. Concurrently, the battery serves as either a standby power source or a source of energy storage, depending on the system's power balance. When the demand from the load exceeds the power supplied by the PV source, the battery provides the additional power needed. When there is excess power being supplied, it is utilised for charging the battery.

All of this is done under the control of a dual-layer controller strategy comprising a PID or MPC and a PWM generator. The output voltage (Vo) is continuously sensed and compared with a reference voltage (Vref), generating an error signal. This error is then fed through the PID/MPC block to calculate the corrective action to be implemented. The controller then instructs the PWM generator to adjust the duty cycles of the converter's switching devices in response. This guarantees that the output voltage of the converter remains stable and accurate despite source or load variations. Filtered power from the converter is then supplied to two separate loads, each of which receives clean and regulated DC power through cascaded filters that eliminate switching transients. The system operates in a feedback-regulated mode around the clock, dynamically managing power flows between the PV, battery, and loads to ensure continuous operation, optimal power utilisation, and overall system efficiency (Figure 2).

Inductor voltage equation:	
$V_{L1} = V_{PV} - V_{bus}(1 - D_1)$	(1)
Output voltage relation:	
$V_{bus} = V_{PV}/(1-D_1)$	(2)
Buck-Boost voltage transfer function:	
$V_{bus} = V_{bat}(D_2 / 1 - D_2)$	(3)
Inductor voltage (L <sub>2</sub> ):	
$V_{L2} = D_2 V_{bat} + (1 - D_2)(-V_{bus})$	(4)
Inductor equation L <sub>3</sub> :	
$V_{Lt} = D_3 V_{bus} + (1 - D_3)(-V_t)$	(5)
Inductor voltage (L <sub>0</sub> ):	
$V_{L0} = V_{bus} - V_{aux}$	(6)

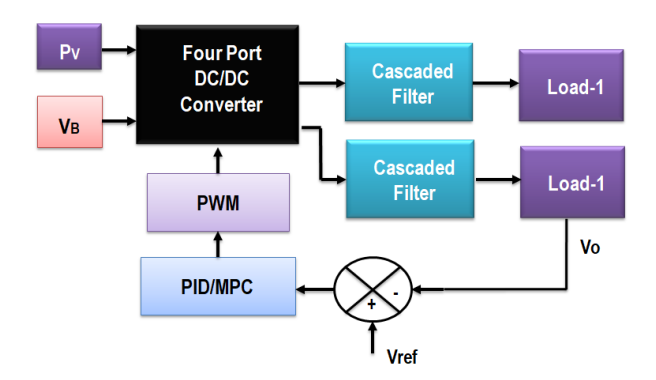


Figure 2: Closed-loop simulation block diagram of a port bi-directional DC-DC converter on behalf of PID/MPC controllers

The Proposed Circuit Diagram of open-loop four-port bi-directional converters with a Cascaded-filter system is shown (Figure 3).

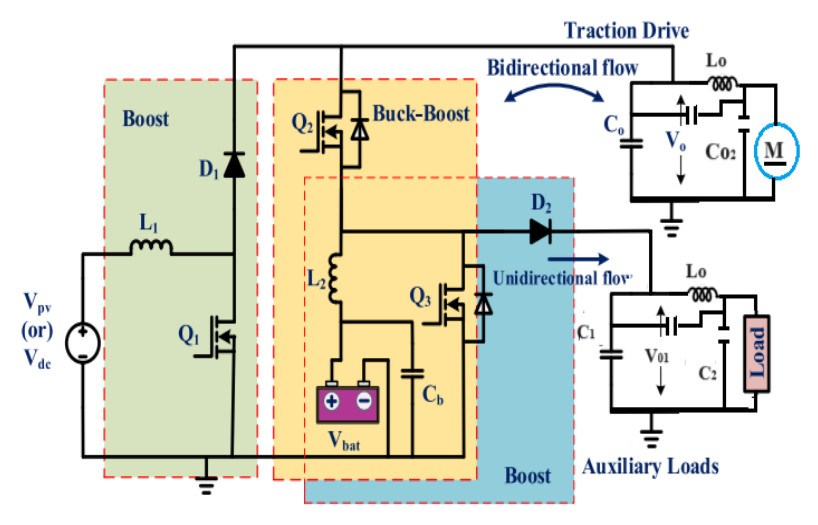


Figure 3: Proposed circuit -diagram of a loop port bidirectional converter along with a cascaded-filter system

The circuit diagram of a closed-loop Port Bi-Directional converter system with an FOPID and SM controller is shown (Figure 4).

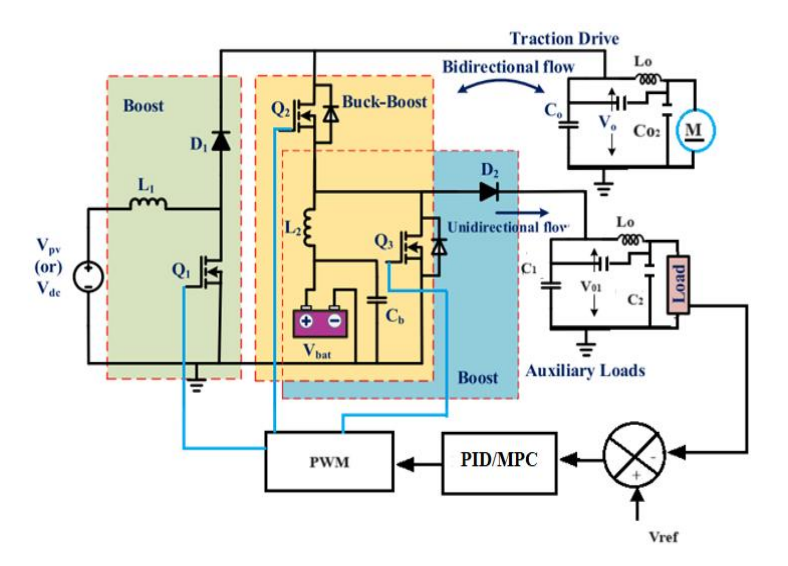


Figure 4: Circuit diagram of closed-loop four-port bi-directional converter system with PID and MP controller

# 3. Simulation Results and Discussion

Simulation parameters of the non-isolated buck boost Port Bi-Directional converter are scheduled in Table 1.

**Table 1:** Simulation parameters of non-isolated buck boost port bi-directional converters

Parameter	Values	
$V_{in}$	15V	
$C_{1}, C_{2}, C_{3}$	50μF	
$C_{5}$ , $C_{6}$ , $C_{7}$	100 μF	
$L_1, L_2$	0.5μΗ	
$L_3$	1.38µH	
$L_4$	1 μΗ	
Frequency	10Khz	
MOSFET	IRF840	
Diode	IN4007	
Resistor	$200\Omega$	
DC motor	38W	
Vo	88V	

The non-isolated buck-boost converter source disturbance circuit diagram is shown in Figure 5. Results are output verification for a four-port bidirectional DC-DC converter system.

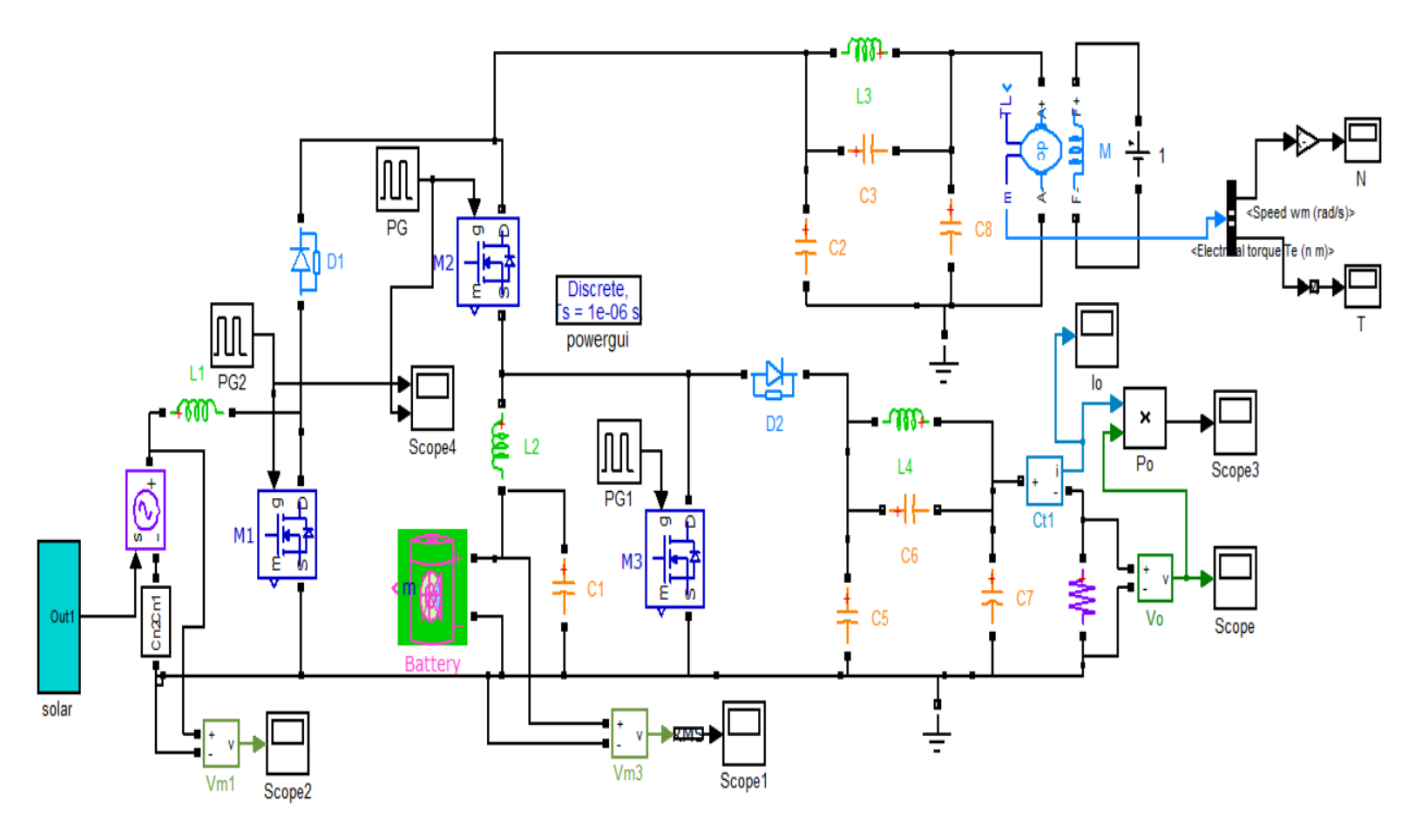


Figure 5: Circuit diagram of a non-isolated buck boost converter with source disturbance system (Case 1)

Verification is obtained using MATLAB/Simulink simulations under three different cases to measure the performance, accuracy, and effectiveness of the control system (Figure 6).

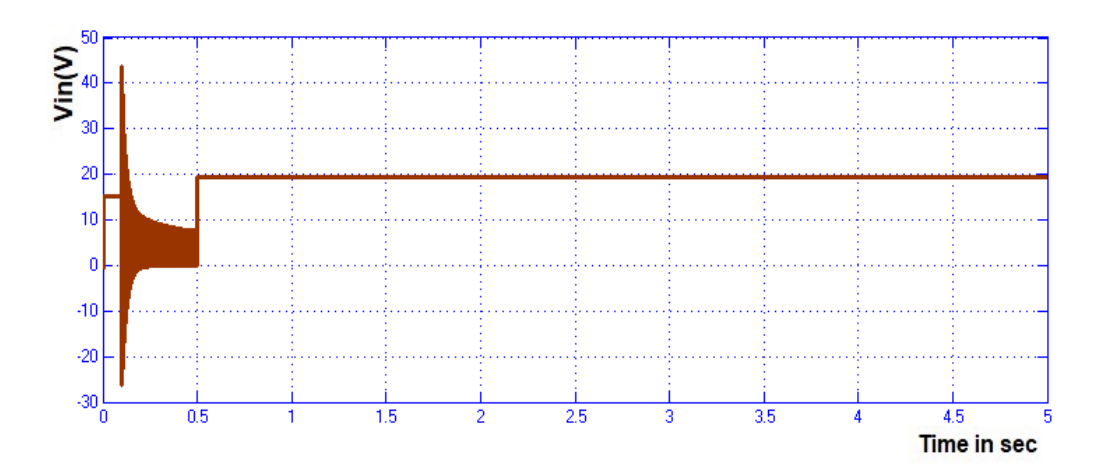


Figure 6: Voltage across PV

Each case represents a different system setup or control mode, and electrical and mechanical parameters consist of observations that determine the converter's capacity to operate effectively under diversified operating conditions (Figure 7).

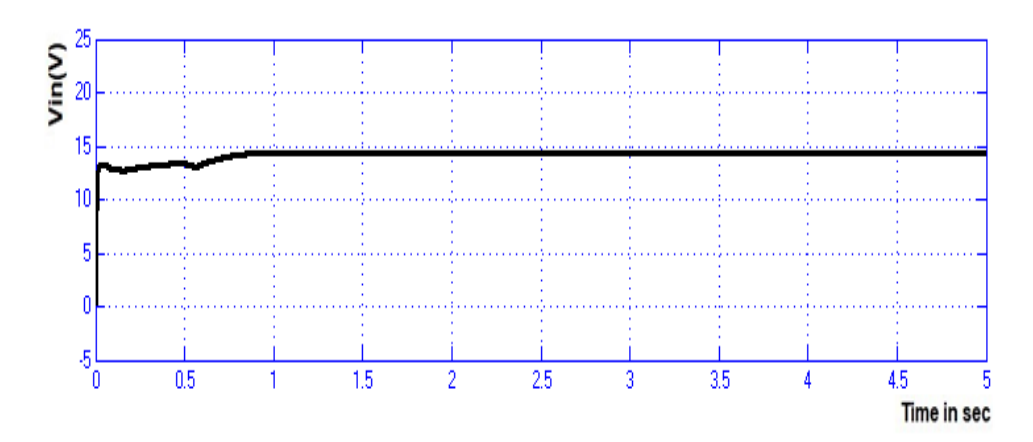


Figure 7: Voltage across battery

In Case 1, the system uses an open-loop or baseline control policy (Figure 8).

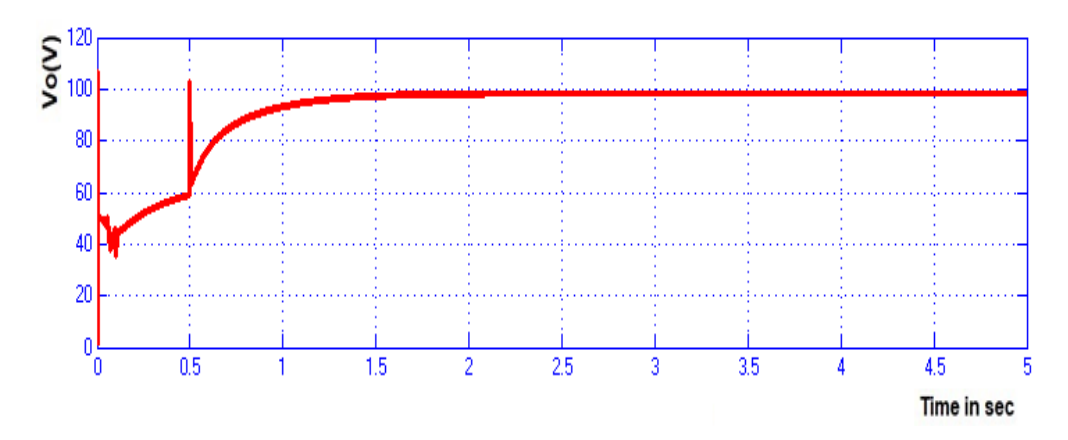


Figure 8: Voltage across R-load

The PV source provides a constant input voltage of 20V, while the battery source supplies a voltage of 15V (Figure 9).

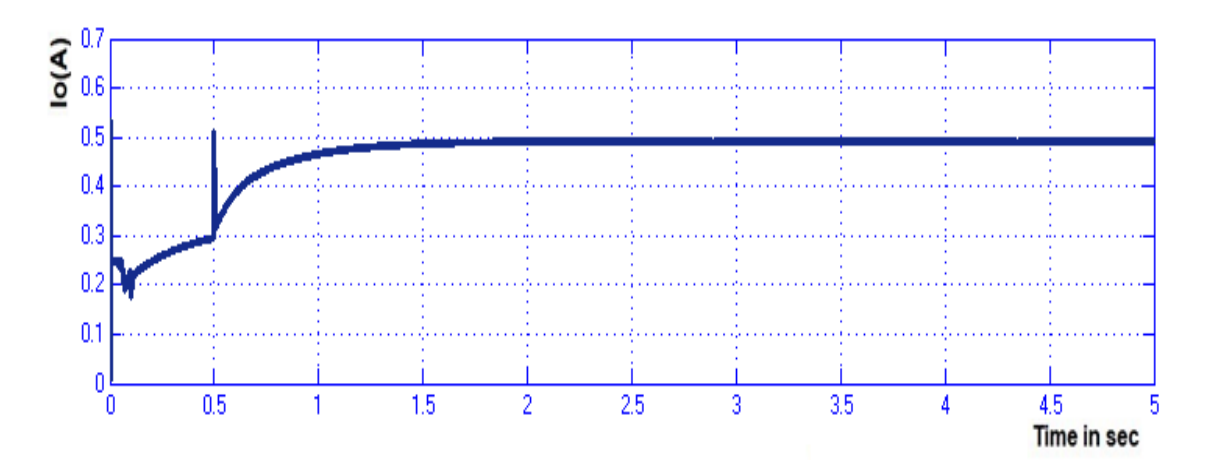


Figure 9: Current throughout the R-load

The converter successfully boosts the voltage, providing an output voltage of 100V on the R-load (Figure 10).

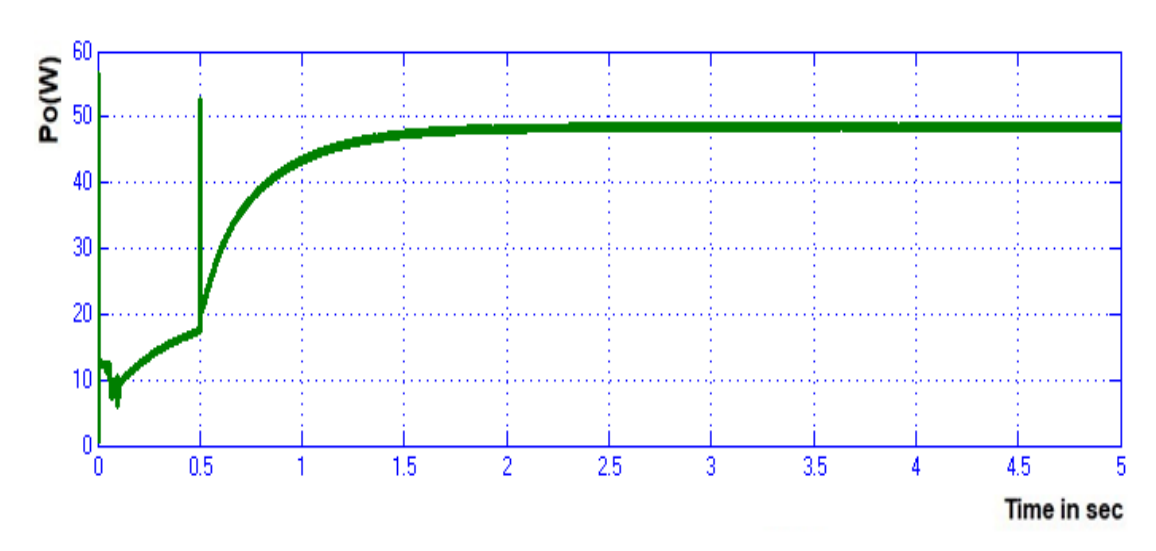


Figure 10: Output-power

The load takes 0.5A of current, representing an output power of 50W, as claimed in the expected power transfer ( $P = V \times I$ ) (Figure 11).

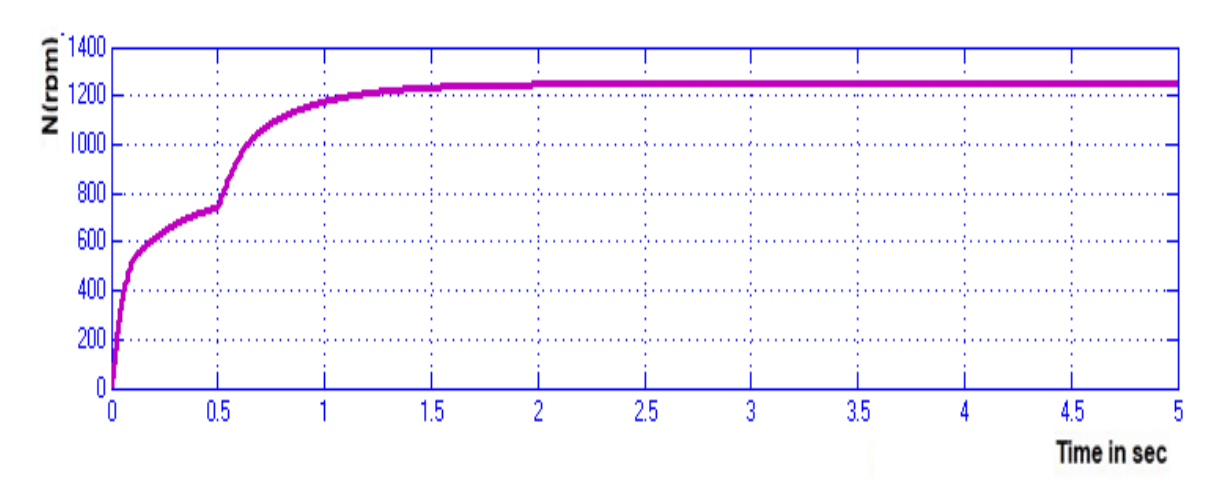


Figure 11: Motor speed

Under such conditions, the motor attached to the system accelerates at a speed of 1210 rpm and produces a torque of 3 Nm (Figure 12).

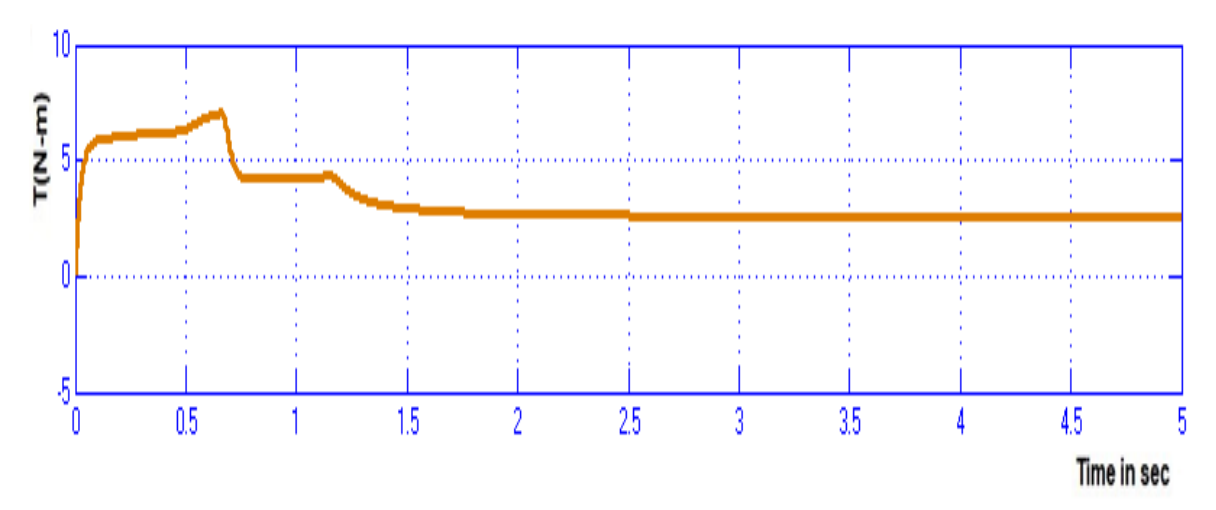


Figure 12: Motor torque

These findings confirm that the baseline converter topology is effective and can provide the necessary power levels to electrical and mechanical loads (Figure 13).

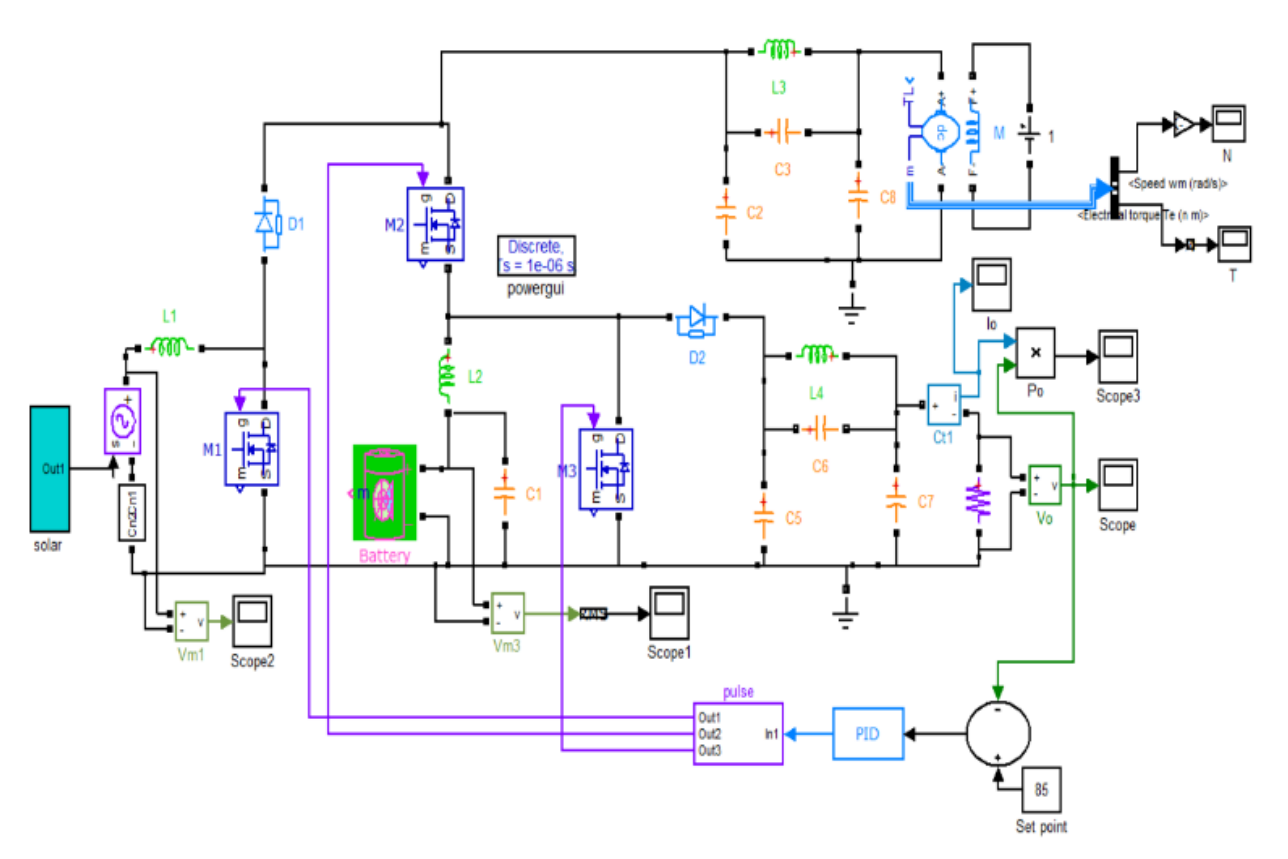


Figure 13: Circuit diagram of non-isolated buck-boost converter with closed-loop PID controller system (case 2)

The circuit diagram of a non-isolated buck-boost converter with a closed-loop FOPID controller system is revealed (Figure 14).

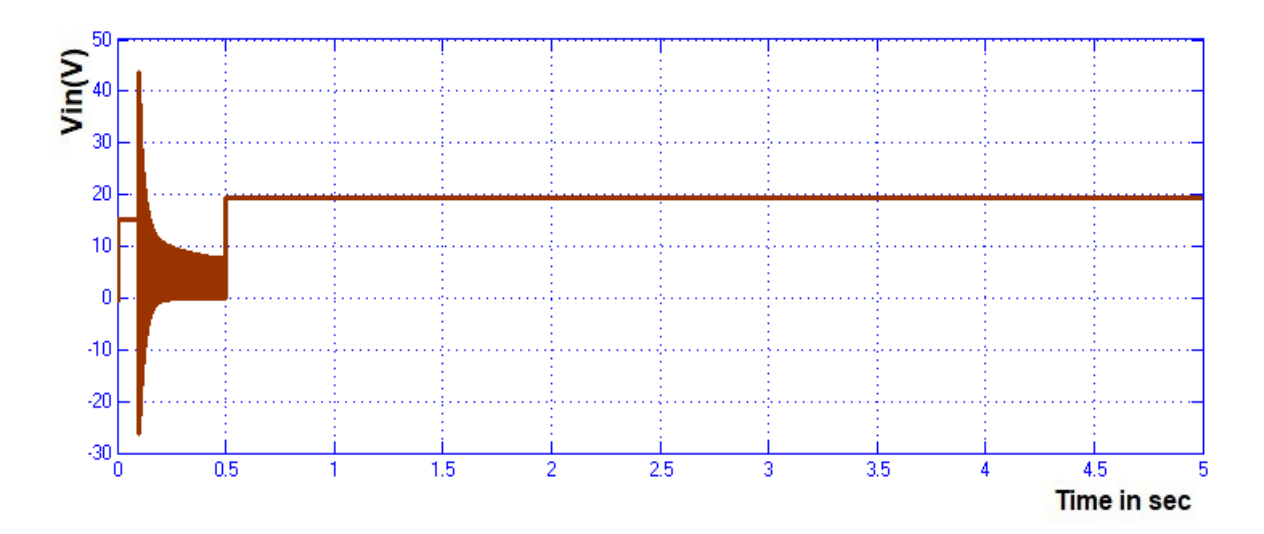


Figure 14: Voltage across PV

Case 2 shows a more sophisticated control technique that includes a Fractional Order Proportional-Integral-Derivative (FOPID) controller (Figure 15).

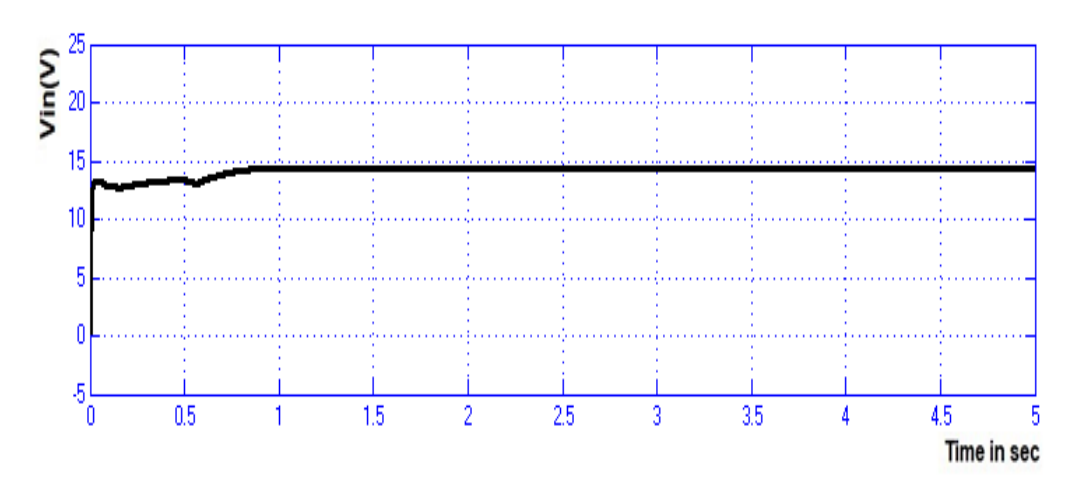


Figure 15: Voltage across battery

The control method is anticipated to provide better stability and performance under dynamic loading (Figure 16).

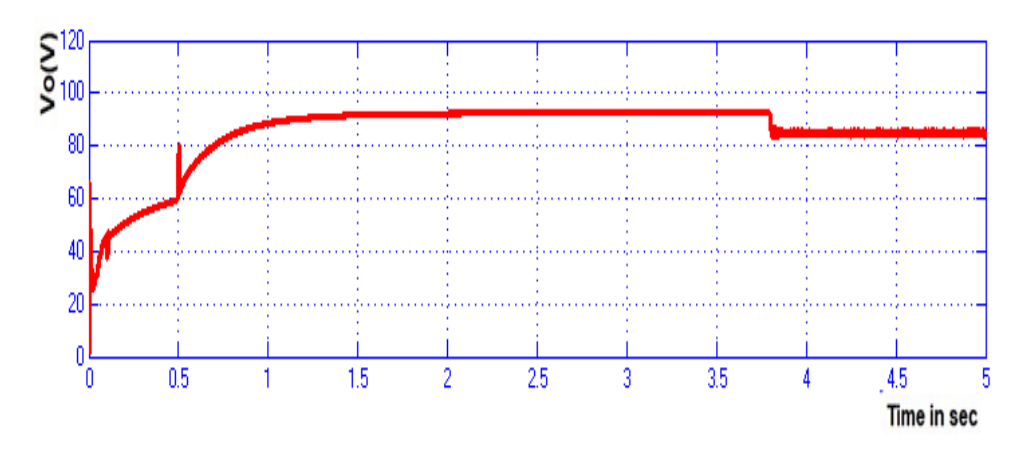


Figure 16: Output voltage across R-load

PV and battery voltage values are the same as 20V and 15V, respectively, i.e., stable input sources (Figure 17).

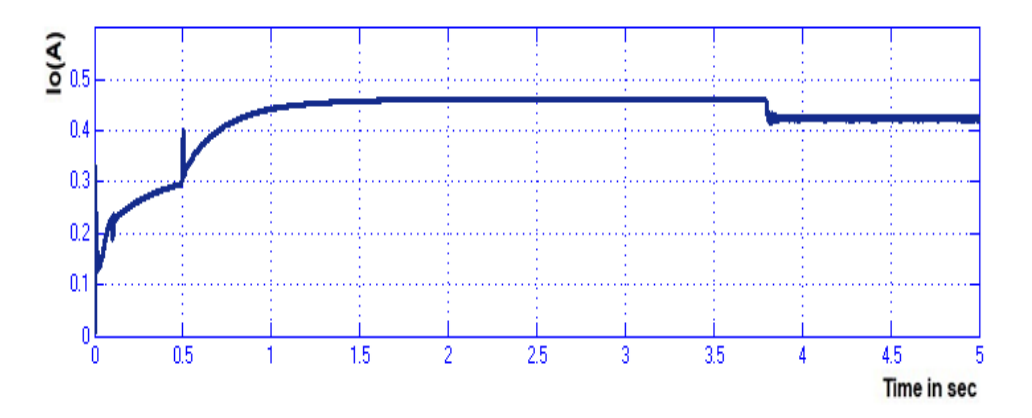


Figure 17: Current throughout the R-load

The voltage across the R-load, however, is lower at 82V, with the current dropping to 0.41A, resulting in a power output of 38W (Figure 18).

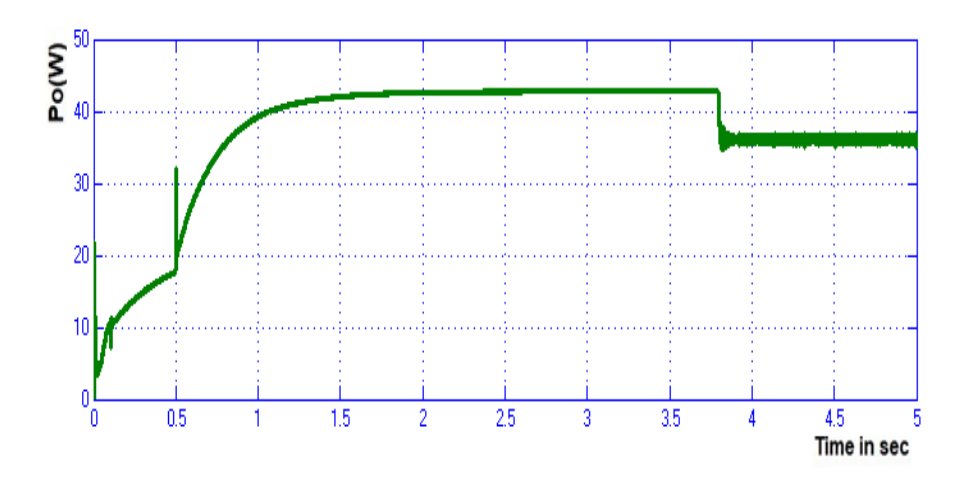


Figure 18: Output power

The speed of the motor for this scenario measures 1050 rpm with a torque output of 2.1 Nm (Figure 19).

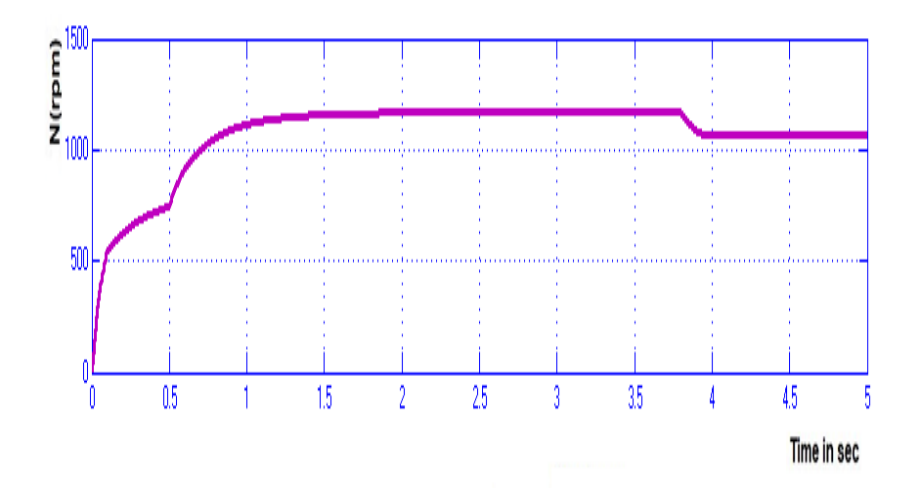


Figure 19: Motor speed

Although these values are slightly lower than those in Case 1, they indicate that the FOPID controller prioritises controlled, stable performance, perhaps at the expense of reduced power (Figure 20).

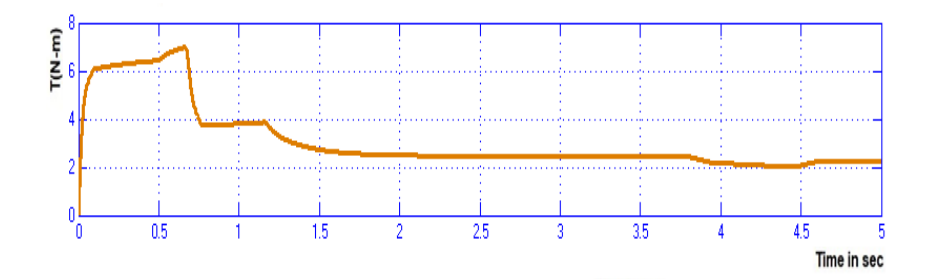
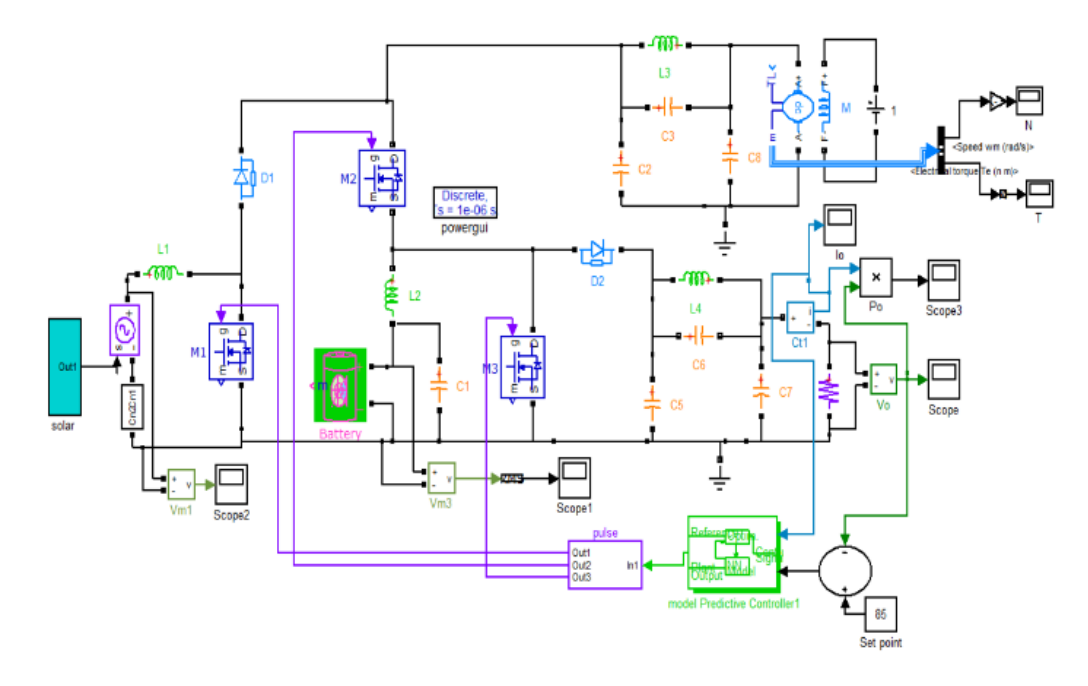


Figure 20: Motor torque

This might be reasonable depending on system objectives like longevity or thermal defence (Figure 21).



**Figure 21:** Circuit diagram of a non-isolated buck-boost converter with a closed-loop model predictive control system (case 3)

The closed-loop non-isolated buck-boost converter circuit-diagram model predictive controller system is revealed (Figure 22).

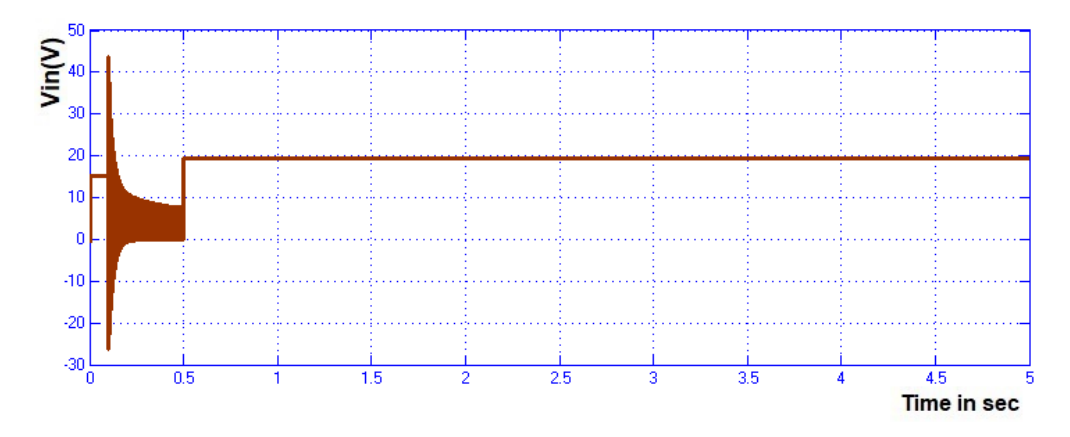


Figure 22: Voltage across PV

Case 3 is a repeat test or a longer test duration under the same conditions as Case 2 (Figure 23).

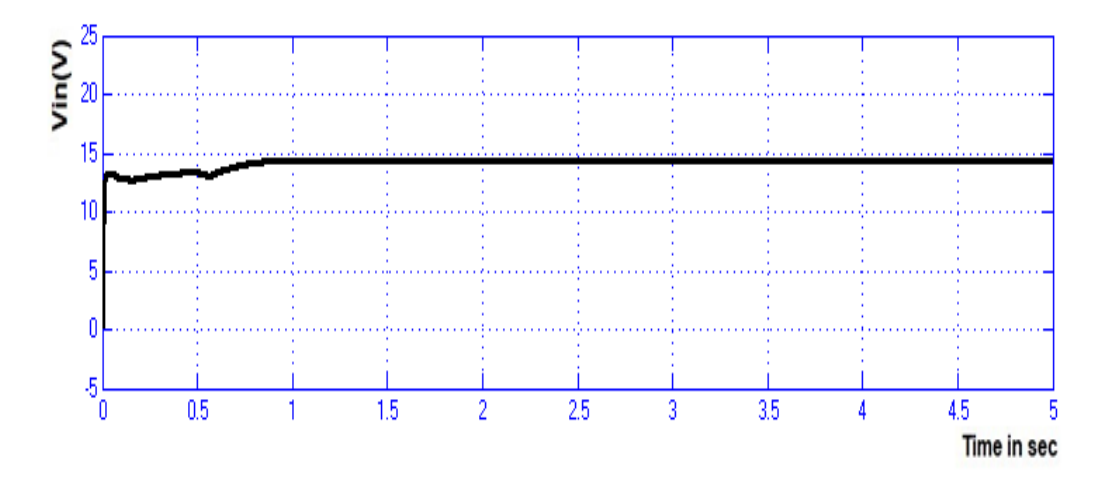


Figure 23: Voltage across battery

Again, the PV and battery voltages are ensured to be 20V and 15V (Figure 24).

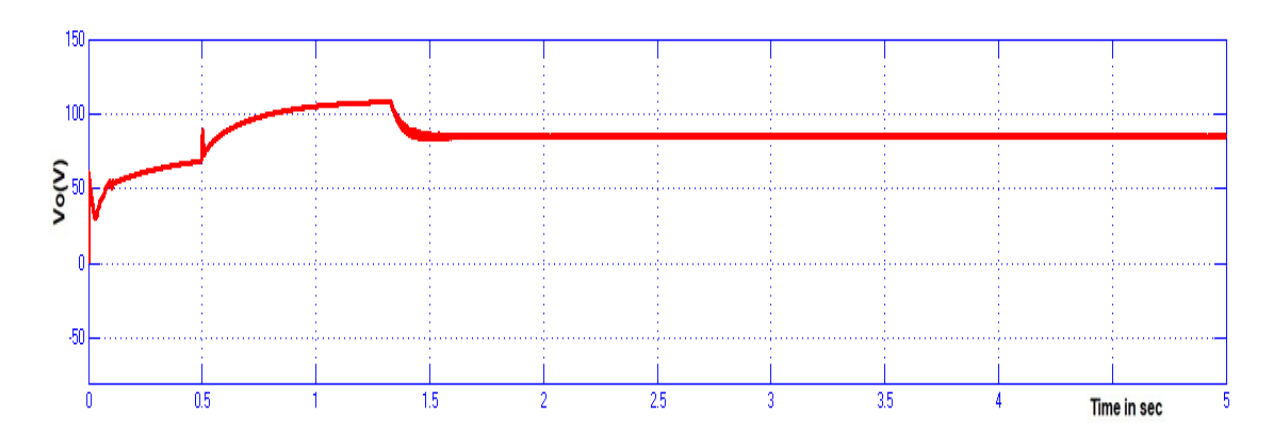


Figure 24: Output voltage across R-load

The R-load shows an output of 82V, current of 0.41A, and power of 38W, which replicates the Case 2 results (Figure 25).

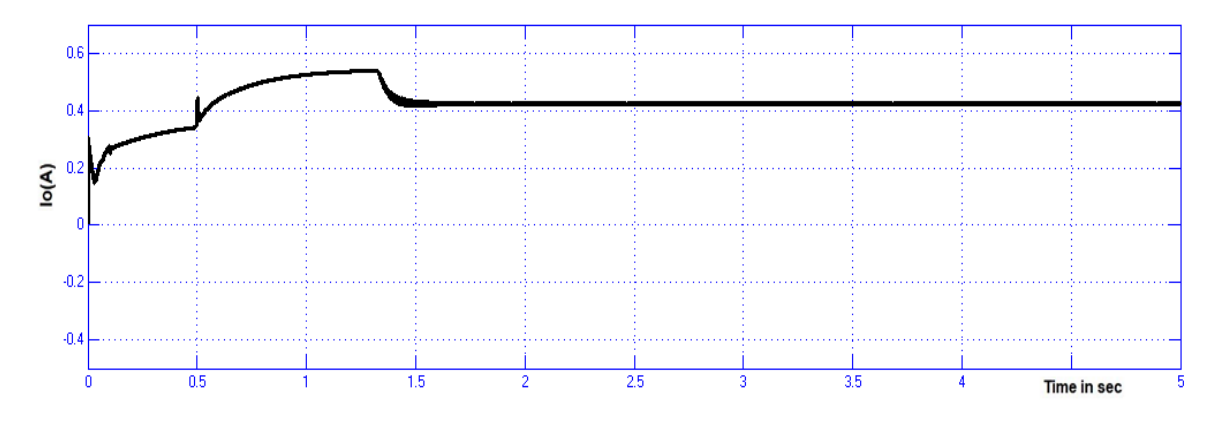


Figure 25: Current throughout the R-load

The motor still delivers 1050 rpm with 2.1 Nm torque (Figure 26).

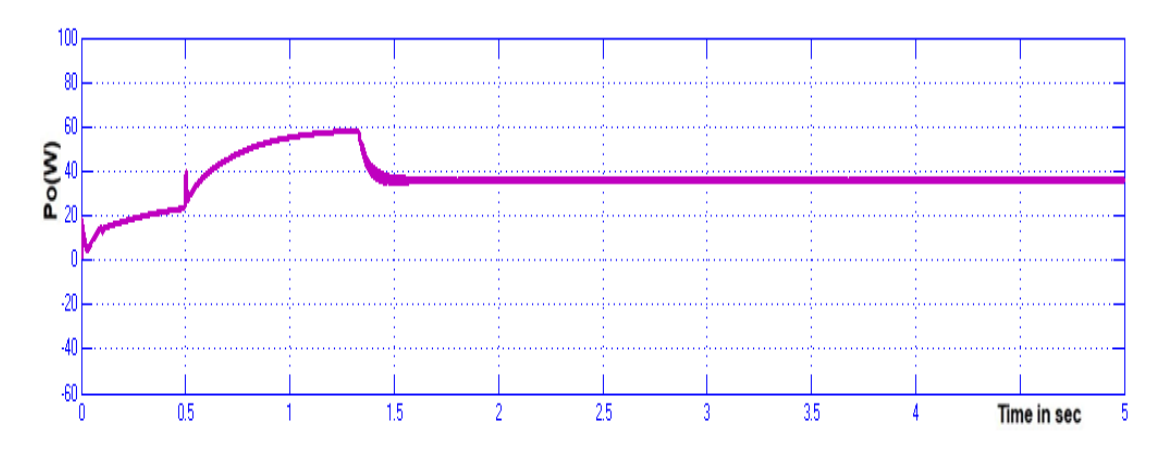


Figure 26: Output-power

The various measurements ensure the system's performance consistency and reliability, even when the control logic is underutilised (Figure 27).

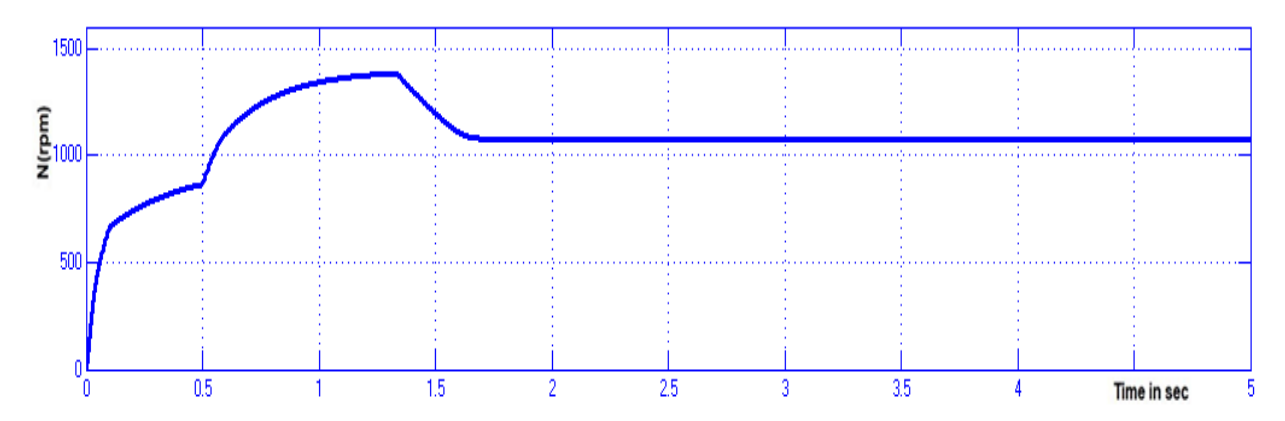


Figure 27: Motor-speed

For all three scenarios, the simulation results not only verify theoretical expectations but also highlight the effect of different control strategies (Figure 28).

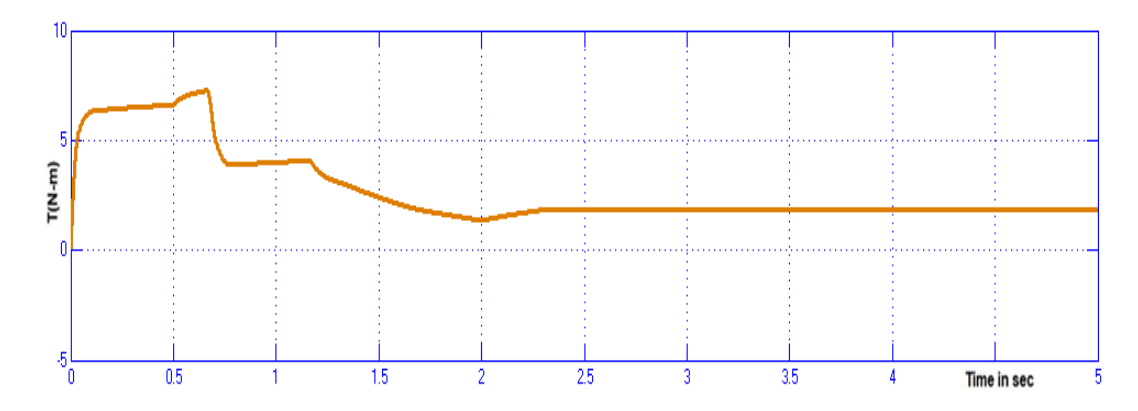


Figure 28: Motor-torque

The comparison of Model Predictive Control (MPC) and PID, as presented in the table and bar chart, once again confirms MPC's superior dynamic response in terms of rise time, peak time, settling time, and steady-state error. This in-depth analysis establishes that the converter system and its control algorithms can provide stable and efficient power under various operating conditions, making them perfectly suitable for renewable energy integration and smart grid applications.

**Table 2:** Comparison time -domain parameters

Controllers	Rise time (s)	Peak time (s)	Setting time (s)	Steady state error (V)
PID	0.60	3.00	3.80	2.56
MPC	0.52	1.30	1.50	0.95

Table 2 provides a comparison of the Time Domain Parameters of closed-loop PID and Model Predictive controllers of a non-isolated buck-boost converter. The results are also confirmed through time-domain analysis, comparing PID and Model Predictive Control (MPC) approaches. Through the comparison, it can be observed that the MPC controller is better than the PID controller in all the critical parameters. In particular, the MPC has a quicker rise time of 0.52 seconds compared to 0.60 seconds for PID, an appreciably quicker peak time of 1.30 seconds compared to 3.00 seconds, and a settling time of only 1.50 seconds compared to 3.80 seconds. In addition, the steady-state error is appreciably smaller with MPC (0.95V) than with PID (2.56V).

The above findings are confirmed by the bar chart plot of the time-domain parameters, which clearly reflects the improved dynamic response of the converter when controlled by an MPC strategy. In general, the simulation results and relative analysis justify the robustness, accuracy, and improved performance of the four-port converter model, especially under model predictive control. Figure 29 shows the bar chart comparison of Time Domain Parameters of closed-loop PID and model predictive controllers for a non-isolated buck-boost converter. From Table 2, it can be observed that the dynamic-response characteristics of a non-isolated buck-boost converter are improved by using a model predictive controller (Figure 29).

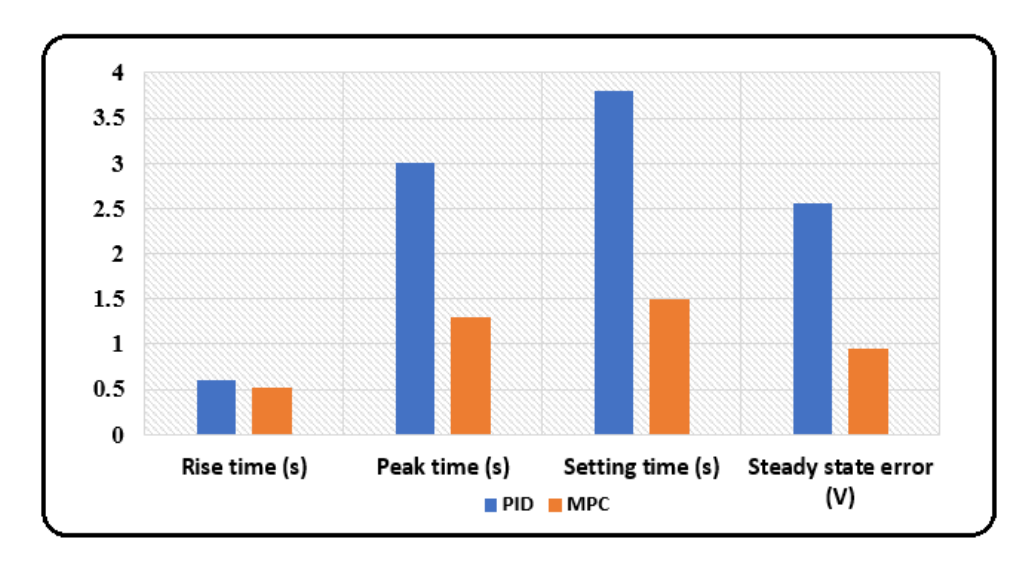


Figure 29: Bar chart comparison of time domain parameters

#### 4. Conclusion

The simulation results clearly show the efficiency of effective control methods in enhancing the dynamic performance of a non-isolated buck-boost converter. Among the controllers that were tested, the conventional PID controller, Model Predictive Controller (MPC), and Sliding Mode Controller (SMC), the SMC developed in a closed-loop system achieves improved control performance. The most important time-domain specifications, such as rise time, peak time, settling time, and steady-state error, are significantly improved using the SMC over the PID controller. For instance, rise time, which is the time it takes for the system output to cross the desired reference voltage for the first time, is decreased from 0.6 seconds with the PID to 0.52 seconds using the MPC with SMC. This more rapid response means the converter can produce the desired output voltage faster, which is critical in power electronics, where the response to load changes or input disturbances needs to be prompt.

The reduction in peak time from 3 seconds to 1.3 seconds further supports this observation, indicating that the system reaches its maximum overshoot much sooner under SMC-based control. Also, the settling time, i.e., the time taken for the system output to stay within a specified error band of the reference, reduces significantly, from 3.8 seconds to 1.5 seconds. This faster settling allows the converter to achieve a stable and constant output voltage earlier, enhancing overall system stability and efficiency. Additionally, the steady-state error is reduced significantly from 2.56 volts to 0.95 volts. A smaller steady-state error implies that the output voltage is very close to the desired voltage, which is of utmost importance in sensitive voltage regulation applications.

The advantage of the Sliding Mode Controller is its robustness and capacity to tolerate system nonlinearities and disturbances. In contrast to the PID controller, which is based on fixed gain parameters and can be taxed by model uncertainties and sudden changes, the SMC forces the system state onto a specified sliding surface with fast convergence and robust disturbance rejection. This robustness renders the SMC extremely suitable for power electronic converters, which are likely to face changing operating conditions and nonlinear dynamics. The comparative analysis indicates that the closed-loop sliding mode control technique is a more effective and reliable solution for non-isolated buck-boost converters.

**Acknowledgement:** The authors extend heartfelt appreciation to the Central University of Tamil Nadu and SRM Institute of Science and Technology for their invaluable support and collaborative spirit that enriched this research endeavour.

**Data Availability Statement:** The data supporting this study are available from the corresponding author upon reasonable request. All authors affirm that the dataset has been used responsibly and in compliance with institutional guidelines.

**Funding Statement:** This research was conducted without any external financial assistance or sponsorship. All authors collectively contributed to the development and completion of the manuscript using their own resources.

**Conflicts of Interest Statement:** The authors declare no conflicts of interest related to this study. The work is an original contribution by the authors, with all sources properly cited and acknowledged.

**Ethics and Consent Statement:** The study was carried out following established ethical standards, with informed consent obtained from all participants and necessary ethical approvals secured prior to data collection.

#### References

- 1. A. A. Saafan, A. Khadkikar, M. S. El Moursi, and H. H. Zeineldin, "A novel non-isolated four-port converter for flexible DC microgrid operation," *IEEE Trans. Ind. Electron*, vol. 71, no. 2, pp. 1653–1664, 2023.
- 2. C. Balaji, S. S. Dash, N. Hari, and P. C. Babu, "A four port non-isolated multi input single output DC-DC converter fed induction motor," in 2017 IEEE 6th International Conference on Renewable Energy Research and Applications (ICRERA), San Diego, California, United States of America, 2017.
- 3. P. I. D. T. Baladuraikannan, J. R. Bindhu, K. Padukolai, and T. Karthikapandi, "Four Port Non-Isolated High Voltage Gain Converter for Renewable Energy Applications," in *Advancement and Research in Instrumentation Engineering, HBRP Publication Pvt. Ltd.*, Chennai, India, 2020.
- 4. Z. Qi, J. Tang, J. Pei, and L. Shan, "Fractional controller design of a DC-DC converter for PEMFC," *IEEE Access*, vol. 8, no. 6, pp. 120134–120144, 2020.
- U. Loganathan, C. Rajeswaran, H. Jayaraj, and M. Magesh, "Optimal fractional order PID controller design of bidirectional DC-DC converter using falcon optimization algorithm," *Int. J. Intell. Eng. Syst.*, vol. 15, no. 3, pp. 333– 342, 2022.
- 6. O. Hegazy, J. Van Mierlo, and P. Lataire, "Analysis, modeling, and implementation of a multidevice interleaved DC/DC converter for fuel cell hybrid electric vehicles," *IEEE Transactions on Power Electronics*, vol. 27, no. 11, pp. 4445–4458, 2012.
- 7. S. Rostami, V. Abbasi, and N. Talebi, "Ultrahigh step-up multiport DC–DC converter with common grounded input ports and continuous input current," *IEEE Trans. Ind. Electron.*, vol. 69, no. 12, pp. 12859–12873, 2022.
- 8. R. Madhana and G. Mani, "Power enhancement methods of renewable energy resources using multiport DC-DC converter: A technical review", *in Sustainable computing: Infomatics system*, Amsterdam, Netherlands, 2022.
- 9. N. Guler and E. Irmak, "Design, implementation and model predictive based control of a mode-changeable DC/DC converter for hybrid renewable energy systems," *ISA Transactions*, vol. 114, no. 8, pp. 1-14, 2021.
- 10. B. Wang, S. Li, S. Kan, and J. Li, "Enhanced tracking of DC-DC buck converter systems using reduced-order extended state observer-based model predictive control," *Journal of Intelligent Systems and Control*, vol. 2, no. 3, pp. 143–152, 2023.